

Article

Study on the Transmission and Evolution Characteristics of Vibration Wave from Vibratory Roller to Filling Materials Based on the Field Test

Changwei Yang ^{1,*}, Liang Zhang ¹ , Yixuan Han ², Degou Cai ³ and Shaowei Wei ³

¹ Department of Civil Engineering, Key Laboratory of High-speed Railway Engineering, Ministry of Education, Southwest Jiaotong University, Chengdu 610031, China; zhangliangDPME@my.swjtu.edu.cn

² Department of Civil Engineering, Beijing Jiaotong University, Beijing 100044, China; HanYixuanBJJD@163.com

³ Railway Engineering Research Institute, China Academy of Railway Sciences, Beijing 100044, China; cdg_cars@163.com (D.C.); wsw_cars@126.com (S.W.)

* Correspondence: yangchangwei@swjtu.edu.cn

Received: 31 January 2020; Accepted: 10 March 2020; Published: 15 March 2020



Abstract: Compaction quality of railroad subgrade relates directly to the stability and safety of train operation, and the core problem of the Intelligent Compaction of railroads is the transmission and evolution characteristics of vibration wave. Aiming at the shortages in exploring the transmission and evolution characteristics of the vibration signal, the typical subgrade compaction project of Jingxiong Intercity Railway Gu'an Station was selected to carry out the field prototypes tests, and the dynamic response from the vibratory roller to filling materials was monitored in the whole compaction process, and some efficient field tests data will be obtained. Based on this, the transmission and evolution characteristics of the vibration wave from the vibratory roller to filling materials in the compaction process are studied from the time domain, frequency domain, jointed time–frequency domain and energy domain by using one new signal analysis technology—Hilbert–Huang Transform. Some conclusions are shown as follows: first, the vibration acceleration peak gradually decreases with the increase of buried depth, and when the buried depth reaches 1.8 m, the vibration acceleration peak is closed to zero. At the same time, when the vibration wave propagates from the wheel to the surface of filling, the attenuation rate of acceleration gradually increases with the increase of rolling compaction times, while the attenuation rate of other layers in different buried depths gradually decreases. Second, the vibration wave contains fundamental wave and multiple harmonics, and the dominant frequency of the fundamental wave is nearly 21 Hz. With the increase of buried depth, the amplitude of fundamental, primary, secondary, until fifth harmonics decreases exponentially and the concrete functional relationship among different amplitudes of harmonics can be summarized as $y = Ae^{-BX}$. Third, the vibration energy focuses on the fundamental wave and primary wave, which can increase with the increase of rolling compaction times, and when the rolling compaction time reaches five, their energy reaches maximum. However, when the filling reaches a dense situation, the energy of the primary wave gradually decreases. Therefore, the maximum rolling compaction time is five in the practical engineering applications, which will be helpful for optimizing the compaction quality control models and providing some support for the development of the Intelligent Compaction theory of railway subgrade.

Keywords: high-speed railway; subgrade compaction; field test; nonlinear transmission mechanism; time–frequency characteristics

1. Introduction

As the foundation of bearing track structure and train, the performance of subgrade is critical to the stability and safety of train operation. With increasing train speeds and axle loads of high-speed trains in China, railroad subgrade is required to have higher strength, stiffness, stability and uniformity. In order to meet these requirements, the main technical measure is that the compaction of railroad subgrade has successful quality control and quality assurance [1–3].

In recent years, researchers have done a lot to control the compaction quality of railroad subgrade. The method of quality control has developed from conventional methods to the Intelligent Compaction (IC) [4–6]. The IC method can monitor the compaction process through a vibratory roller equipped with accelerometers, and feedback compaction information to the control system in real-time. By analyzing the vibration characteristics of vibratory roller and filling materials, several compaction values that can reflect the compaction quality were proposed [7]. For instance, Compaction Meter Value (CMV) [8,9], which is the amplitude ratio of the first harmonic wave to the fundamental wave obtained through spectral analysis of the measured vertical acceleration, was applied to control the compaction quality of subgrade and dam. On the basis of CMV, Compaction Control Value (CCV) [10], which further considers the influence of half-order harmonics and higher-order harmonics, was proposed. Total Harmonic Distortion (THD) [11] and Resonant Meter Value (RMV) [6] are similar to CCV. In addition, Machine Drive Power (MDP) [12] is calculated by analyzing the energy needed to overcome the resistance of the vibratory roller when it moves, and it is often used in combination with CMV in some projects [4,13]. The application of these compaction measurement values avoided over- or under-compaction of filling materials, and improved the efficiency of subgrade compaction [6,14,15]. However, the vibration wave is very complicated and its transmission and evolution mechanism is not clear enough [16,17], especially in the construction field, which leads to that CMV can only be used to roughly estimate the compaction quality of subgrade and the above-mentioned other (CCV, THD, RMV and MDP) compaction measurement values also had some problems in practical applications [18–21]. Therefore, it is very necessary to study the transmission and evolution characteristics of the vibration signal from the vibratory roller to filling materials in the compaction process.

In exploring the transmission and evolution characteristics of the vibration signal, two approaches have been used: (1) analyses were performed in the time domain, but only vibration time-history responses were obtained [8,22–24]; (2) analyses were performed in the frequency, but only Fourier spectrums and energy spectrums are obtained [25–29]. However, the vibration wave is a complicated nonlinear non-stationary signal and its vibration frequency and amplitude are constantly changing in the compaction progress. Its order of harmonics cannot be predicted, which will affect the analysis accuracy if it is calculated from the time domain or the frequency domain alone [30–32]. Therefore, the jointed time–frequency domain will be a better approach for studying the transmission and evolution characteristics of the vibration signal from the vibratory roller to filling materials in the compaction process. Few studies have been done by using the jointed time–frequency domain to study the transmission and evolution characteristics of the vibration signal. At the same time, a lot of research mainly relies on numerical simulation, theoretical analysis and laboratory tests [33–35], and few field prototypes tests have been done because of its high cost, long period and so on. However, usually, there are some assumed conditions or limiting conditions in the numerical simulation, theoretical analysis and laboratory tests, which will limit the application of research results [36–39].

Therefore, the typical subgrade compaction project of Jingxiong Intercity Railway Gu'an Station is selected to carry out the field prototypes tests, and the dynamic response from the vibratory roller to filling materials was monitored in the whole compaction process, and some efficient field tests data will be obtained. Based on this, the transmission and evolution characteristics of the vibration signal from the vibratory roller to filling materials in the compaction process are studied from time domain, frequency domain, jointed time–frequency domain and energy domain by using one new signal analysis technology, Hilbert–Huang Transform, which can relatively overall reveal the transmission and evolution mechanism of vibration wave. The research results will be helpful for optimizing the

compaction quality control models and providing some support for the development of the Intelligent Compaction theory of railway subgrade.

2. In Situ Test Overview

2.1. Test Section Information

This paper took the Jingxiong Intercity Railway Gu'an Station with a large number of subgrade compaction work as the test section, and the planed test site is 200 m in length and 100 m in width, as shown in Figure 1. The filling part is the embankment part below the subgrade bed surface, which is divided into 19 layers. The thickness of each layer is controlled at about 30 cm. The coarse breccia of groups A and B with a dry density of 2.3 g/m^3 and an optimal moisture content of 5.2% was used to fill subgrade, and its particle grading curve is shown in Figure 2.



Figure 1. Test section.

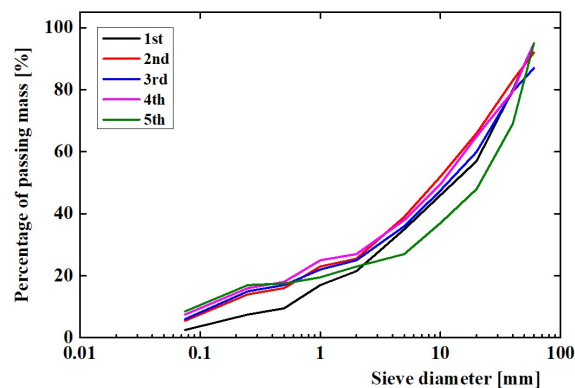


Figure 2. The particle grading curve of filling materials.

2.2. Test Equipment

A San-Yi Heavy Industry single-wheel (Type SSR260C-6) vibratory roller was used for this research study. The total weight of the compactor is 26.7 t. It can provide circular excitation over a frequency range of 27–31 Hz and an amplitude range of 1.03–2.05 mm. The vibration characteristics of wheel and filling materials were monitored using $\pm 5 \text{ g}$ and $\pm 16 \text{ g}$ accelerometers, which could record three vibrations (x -axis, y -axis and z -axis) in mutually perpendicular directions, as shown in Figure 3. The data in the test was captured via a 32-bit data acquisition system (Type DH5922D). In order to ensure the fit between the collected signal and the original signal, the sampling frequency of acceleration sensors was set to 2000 Hz. All the data acquisition systems and sensors were calibrated before the test.

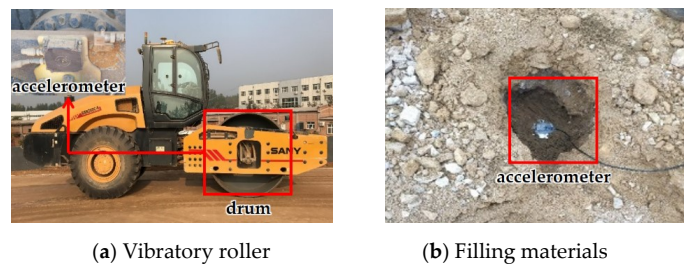


Figure 3. Accelerometers used in the test.

2.3. Test Design

In order to collect the vibration signals during the compaction process, the measurement points are, respectively, arranged on the vibratory roller and different filling layers. As shown in Figure 4, one measurement point was arranged on the vibration wheel, and 12 measurement points were arranged on filling materials. The measuring points in filling materials were arranged on the upper and lower surfaces of each layer to monitor the transmission of the vibration signals at the interface. All filling layers were compacted except for the first layer. Based on a large number of compaction work in the early stage, the weak vibration mode of vibratory roller was more conducive to the compaction of this filling material. Consequently, when filling materials of the first layer are flattened and statically pressed, eight times compaction is carried out by means of weak vibration mode. Lightweight deflectometer (LWD) is used to measure the properties of filling material after each compaction [40].

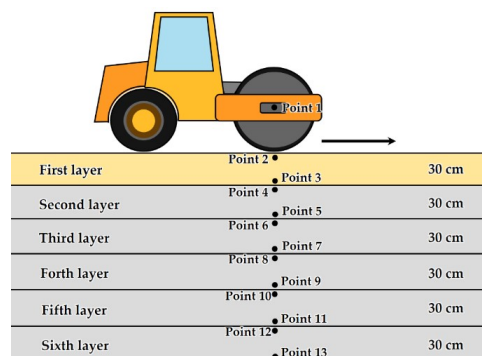


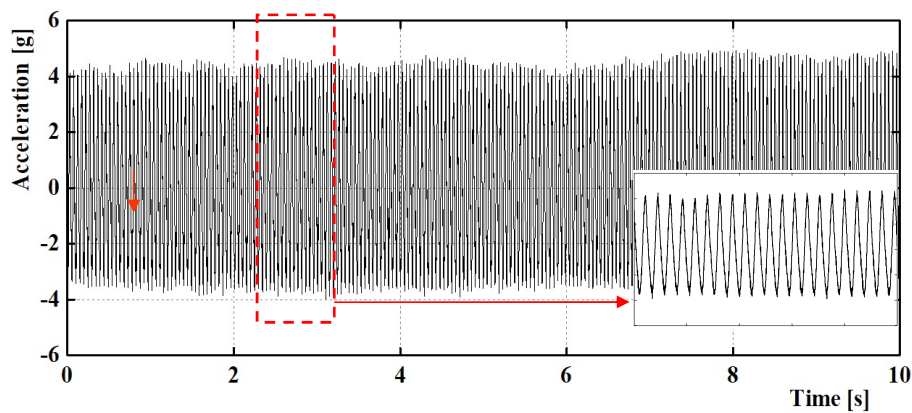
Figure 4. The distribution of the measurement points.

3. Test Results and Analysis

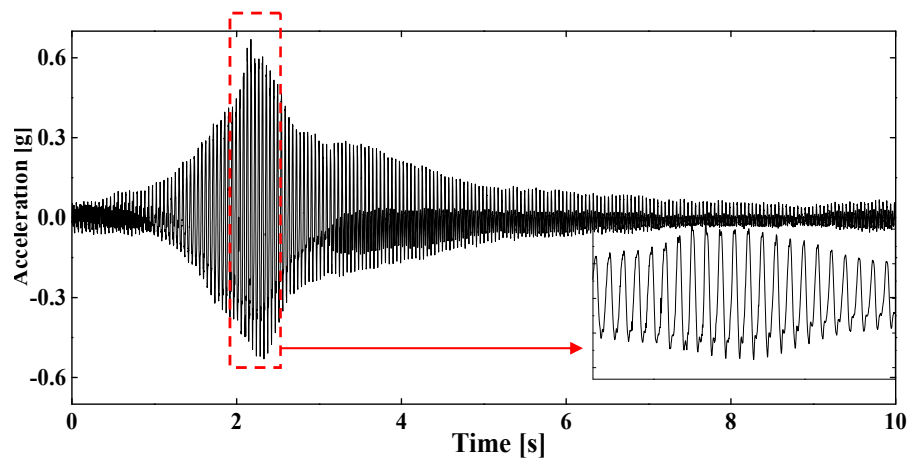
3.1. Analysis of Peak Attenuation Law of Vibration Acceleration

The peak acceleration in the vibration signal reflects the vibration response between the vibratory roller and filling materials. Under the action of the vibratory roller, the vibration response time of the filling materials is about 10s and the peak acceleration of the wheel is about eight times that of the first layer, as shown in Figure 5. Figure 6 shows the variation curve of the peak acceleration with the number of rolling compaction times for each measuring point. It can be found the peak acceleration of the vibration signal was gradually decreased during the propagation of the vibration signal from the vibratory roller to the deep filling layer, which is approximately inversely proportional to the depth. However, the peak acceleration does not decrease linearly, nor does it increase at the interface of different filling layers. The reason may be that the difference in the physical and mechanical parameters of filling materials on both sides of the interface results in the reflection of the vibration signal at the interface [41]. In addition, the peak acceleration of each measuring point increases with the increase of the number of rolling compaction times and reaches the maximum value in the fifth compaction. At this time, the peak acceleration of the wheel keeps around 6.06 g, and the peak acceleration of the first layer keeps around 2.06 g. The LWD detection value of the filling materials also tends to be stable

after the fifth compaction, indicating that the peak attenuation law of the vibration signal is related to the soil compactness.



(a) Measurement Point 1



(b) Measurement Point 3

Figure 5. Acceleration time-history curves.

In order to further quantify and analyze the attenuation law of the vibration signal from the vibration wheel to the deep filler, this paper divides the peak acceleration difference between the filling materials and the wheel by the peak acceleration of the wheel as the attenuation rate, as shown in Figure 7.

According to Figure 7, it can be found that the peak attenuation rate of acceleration is the largest when the vibration signal is transmitted from the wheel to the surface of filling materials. With the increase of compaction times, the attenuation rate increases from 51% to 66%. As the stiffness of the filling materials increases, the vibration signal has to consume more energy for transmission to the filling layer. The transmission mechanism of the vibration signal from the shallow filling layer to the deep filling layer is the opposite. As the filler enters the dense state from the loose state, the stiffness between different layers gradually decreases so that the peak attenuation rate of the vibration signal also gradually decreases. The attenuation rate of the vibration signal transmitted to the fourth layer (1.2 m) is more than 90%. It can be seen that the critical depth of the vibration acceleration in the filling layer is about 1.2 m.

3.2. Acceleration Spectrum Analysis

The variation of the vibration signal spectrum is related to the stiffness of the filling materials under compaction [42,43]. Thus, the Fast Fourier Transform (FFT) was used to decompose the vibration

signal into the frequency domain in order to analyze the frequency information, as shown in Figure 8. It can be seen that the frequency and amplitude of the fundamental wave and multiple harmonic waves appear in the acceleration of each measuring point. The fundamental wave frequency of the vibration acceleration is basically stable near 21 Hz during the compaction process, and the fundamental wave frequency increases slightly from the vibration wheel to the filler surface, maintaining stability in each filling layer.

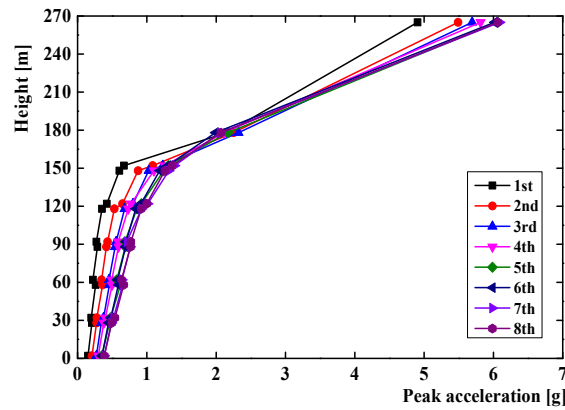


Figure 6. Peak acceleration of each measuring point.

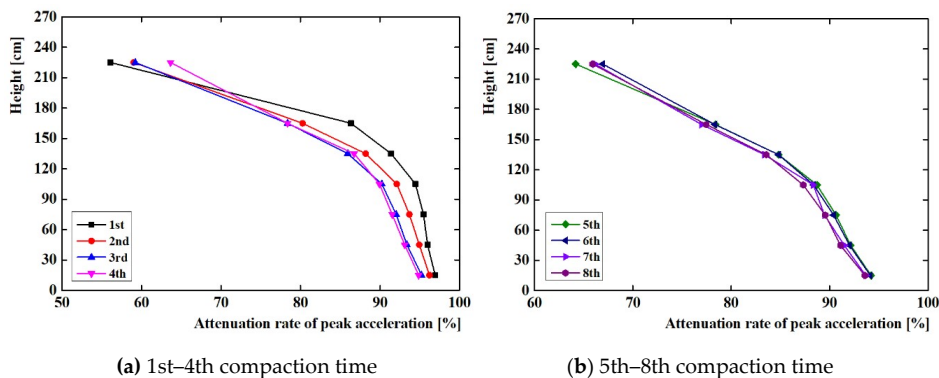


Figure 7. Peak attenuation rate of acceleration of each measuring point.

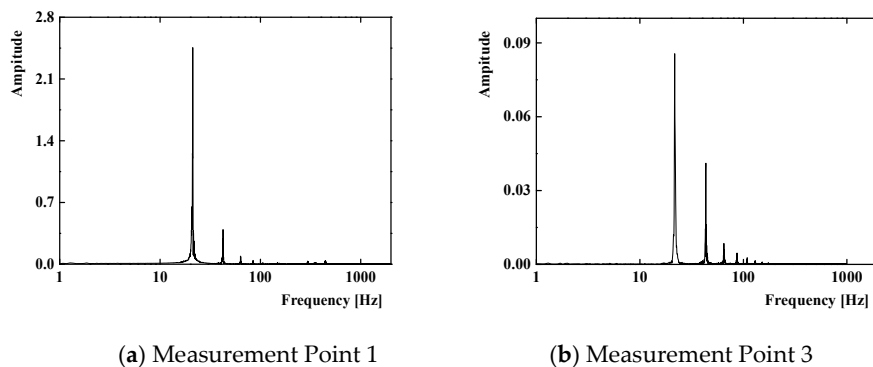
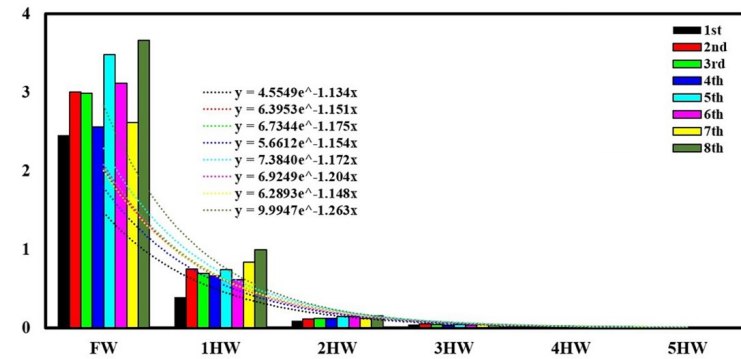


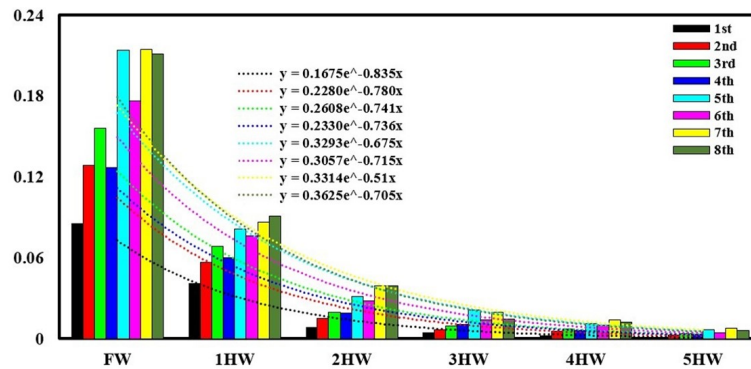
Figure 8. Fourier spectrum.

Figure 9 shows the variation of fundamental and multiple harmonic amplitudes of each measuring point in the compaction process. When the vibration signal propagates from the vibration wheel to the deep layer, the ratio of fundamental amplitude to total amplitude decreases with the increase of buried depth. With the increase of buried depth, the amplitude of fundamental, primary, secondary, until fifth harmonics decreases exponentially, and the attenuation models are shown in Figure 9.

The concrete functional relationship among different amplitudes of harmonics can be summarized as shown: $y = Ae^{-BX}$. In the formula, A and B represent the coefficient, X represents the order of harmonic and Y represents the amplitude of harmonic when its order is X.



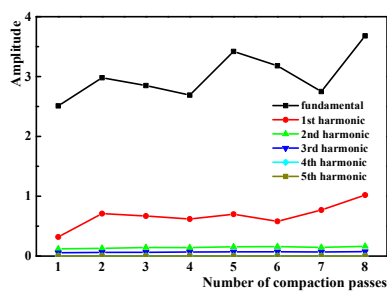
(a) Measuring Point 1



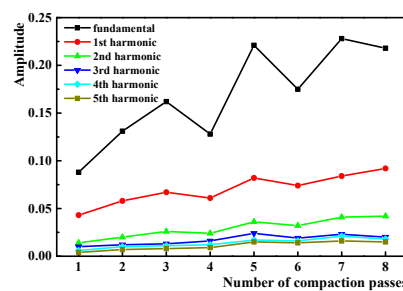
(b) Measuring Point 3

Figure 9. Variations of the fundamental and multiple harmonic amplitudes of each measuring point.

Figure 10 shows the relationship between the amplitude of harmonic and rolling compaction times, which shows that with the increase of compactions passes, the amplitudes of the fundamental wave and the multiple harmonic waves generally show a trend of “increase → decrease → increase”, and the decrease of amplitude occurs in the sixth pass compaction process.



(a) Measuring Point 1



(b) Measuring Point 3

Figure 10. Relationship between amplitude of harmonic and rolling compaction times.

3.3. Time–Frequency Characteristic Analysis

The Hilbert–Huang transform (HHT) method was used to analyze the characteristics of the vibration signals in the joint time–frequency domain. The HHT method is a self-adaptive time–frequency

analysis method suitable for nonlinear and unstable signal processing proposed by Huang [44,45], which mainly includes two parts: EMD empirical mode decomposition and Hilbert spectrum analysis.

The EMD method assumes that any signal is a composite signal composed of different Intrinsic Modal Functions (IMFs), and each IMF component must meet two conditions: (1) the number of extreme points and zero-crossing points were the same or at most one difference; (2) the mean of the upper and lower envelope of the signal was zero. In this way, any signal can be decomposed into multiple IMFs [44].

Then, for vibration signal $F(t)$, which was decomposed into multiple IMFs, its Hilbert transformation is as follows:

$$G(t) = \frac{1}{\pi} K \int_{-\infty}^{\infty} \frac{F(\delta)}{t - \delta} d\delta$$

where K is a Cauchy principal value. Established analytic signal $P(t)$:

$$P(t) = F(t) + jG(t) = a(t)e^{j\Phi(t)}$$

where $a(t)$ is the amplitude function and $\Phi(t)$ is the phase function.

$$a(t) = \sqrt{F^2(t) + G^2(t)}$$

$$\Phi(t) = \arctan \frac{G(t)}{F(t)}$$

The instantaneous frequency of the signal could be obtained by differentiating the phase [45]. Therefore, the Hilbert transform of the decomposed IMF component can obtain the distribution law of the signal on the time–frequency energy scale, which is the form of the Hilbert spectrum:

$$H(\omega, t) = \operatorname{Re} \sum_{i=1}^{n+1} a_i(t) \cdot e^{j \int \omega - i(t) dt}$$

By integrating the time in the expression formula of the Hilbert spectrum, the distribution law of the signal on the frequency–amplitude scale can be obtained, which is the form of the corresponding marginal spectrum:

$$h(\omega, t) = \int_{-\infty}^{\infty} H(\omega, t) dt$$

Taking the acceleration of the first compaction vibrating wheel (Measuring Point 1) as an example, the original vibration signal is decomposed by EMD to obtain each IMF component, as shown in Figure 10. Fourier transform is used to obtain the spectrum curve of each IMF component, as shown in Figure 11. From Figures 10 and 11, the original vibration signal of the wheel is decomposed into 13 IMF components and one residual component, and each IMF component has a different amplitude and frequency component. Among each IMF component, the waveform of IMF6 is consistent with that of original signal, and its dominant frequency and amplitude are substantially consistent with that of the original signal; IMF5 mainly contains the same frequency as the fundamental wave, first a harmonic wave and second harmonic wave, but its dominant frequency and amplitude are the closest to the first harmonic. The three frequencies with the largest amplitude of IMF4 are basically consistent with the frequencies and amplitudes of second, third and fourth harmonic waves of the original vibration signal, and the remaining components are high-frequency or low-frequency interference signals. Therefore, the waveform of the wheel is composed of IMF6, IMF5 and IMF4. To some extent, EMD can identify the fundamental and harmonic components of vibration signals, and remove the mechanical and environmental noise interference.

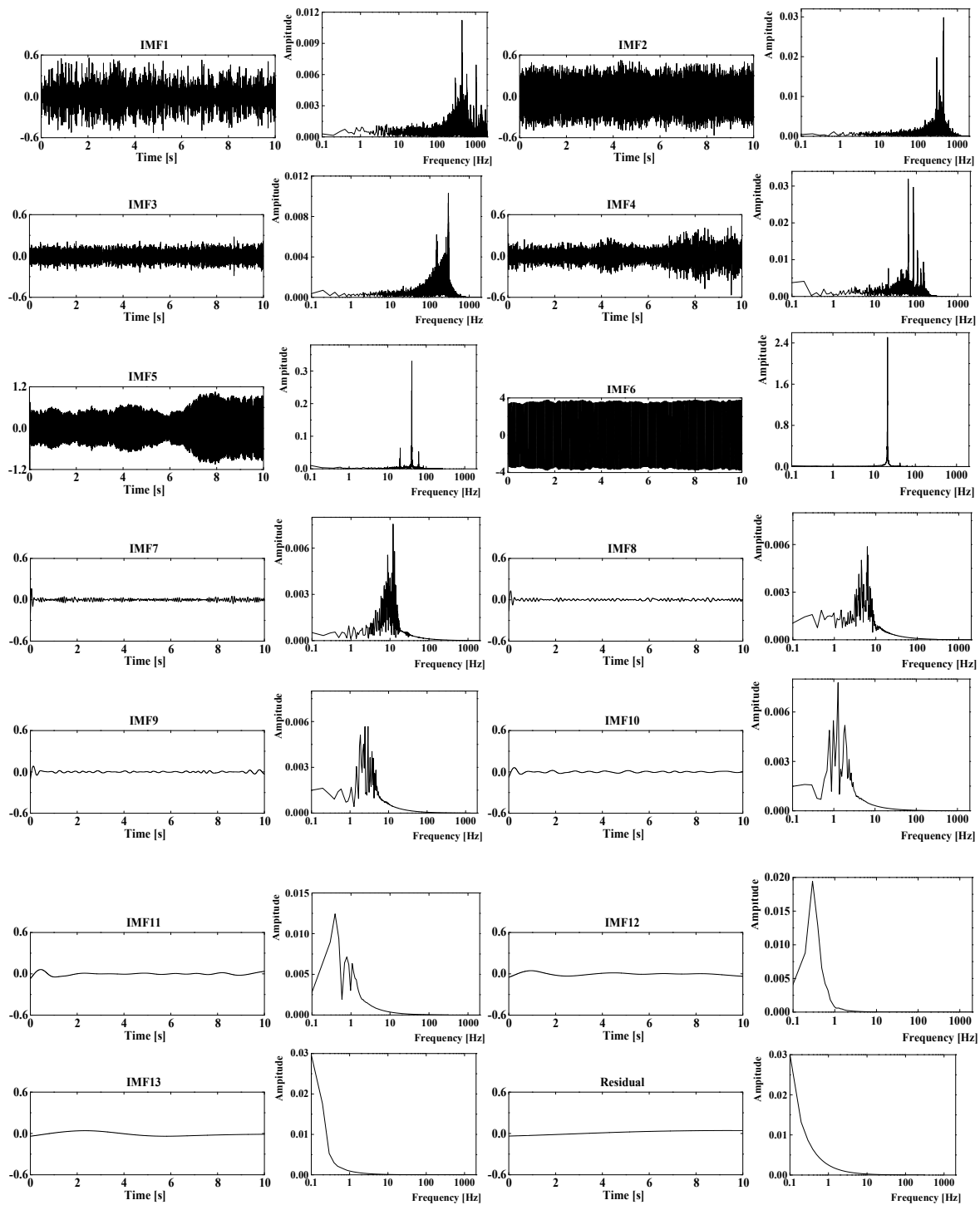
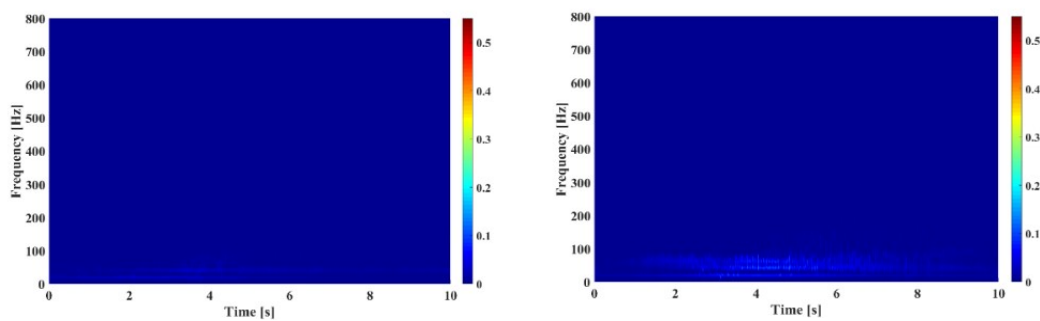


Figure 11. Intrinsic Modal Function (IMF) components and their Fourier spectrums.

Based on the results of EMD, the energy spectrum is obtained by Hilbert transform, and the evolution characteristics of the vibration signal energy in the time–frequency domain are represented by a two-dimensional plane contour map, and Figure 12 is the Hilbert energy spectrum of each measuring point in the first pass and the eighth pass. According to the comprehensive analysis of Figure 12, it can be found that the evolution characteristics of the vibration signal can be better described by the Hilbert–Huang transform, and the vibration energy carried by the vibration wave from top to bottom is gradually reduced. During the first pass compaction process, the vibration energy of the wheel varies little from $T = 0$ s to $T = 10.0$ s, mainly distributed between the fundamental wave frequency of 20 and

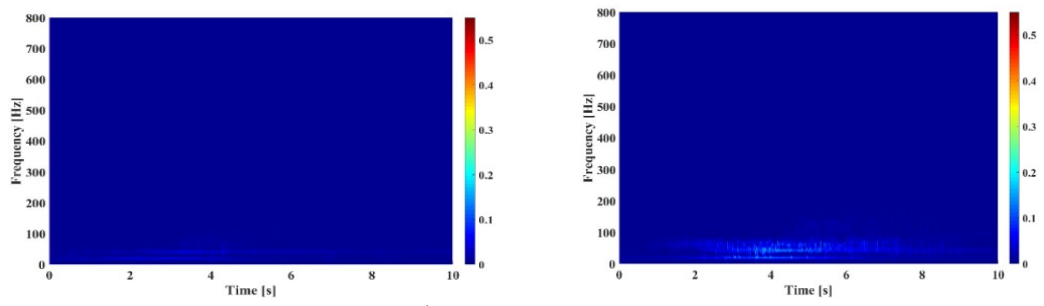
30 Hz, and a small amount is distributed between 40 and 50 Hz of the first harmonic wave frequency. The energy carried by each measuring point of the filling layer is concentrated between $T = 2$ s and $T = 3$ s when filling materials are loose, and also distributed near the frequency corresponding to the fundamental wave and the first harmonic in the frequency domain. With the increase of compaction times, the density of filling material increases, the vibration energy of the wheel and each measuring point of filling material increases obviously, and the action time increases from 1s to 2 s, but the distribution in the frequency domain does not change much, which shows that the effective rolling time of the vibrating roller increases gradually during the compaction process of the filling material.

Based on the Hilbert spectrum, the marginal spectrum of each measurement point is obtained in order to further analyze the distribution of vibration energy on the frequency-amplitude scale. Figure 13 shows the variation of the Hilbert marginal spectrum of each point of wheel and filling materials during the compaction process. It can be found that the vibration energy of each measuring point is mainly concentrated between 10 and 100 Hz, of which the vibration energy of wheel is mainly distributed at the frequency corresponding to the fundamental wave and partially distributed at the frequency corresponding to the first harmonic wave, while the vibration energy has little difference in the distribution of the fundamental wave of the filler and the frequency corresponding to the first harmonic wave. A small amount is distributed in the frequency corresponding to the third harmonic wave. As the number of rolling compaction times increases, the vibration energy carried by the fundamental wave and the first harmonic wave of the wheel increases continuously, similar to the acceleration peak, and tends to be stable after the fifth pass compaction reaches the maximum value. In the filling, the energy carried by the vibration signal began to decrease after the fifth compaction, especially the peak value of the amplitude of the first measuring point, which decreased by about 0.1. It shows that the energy carried by vibration signal gradually transfers from fundamental wave to higher harmonic wave with the increase of filling materials stiffness. When the number of compaction times is increased, the compaction energy increases gradually, but the difference is small with the fifth compaction. It shows that the vibration energy of the receiving wheel in the first layer is less than that in the loose state after compaction, and the transmission loss of the vibration energy in this layer is also reduced. The change of the rigidity and damping of the filling materials mainly affects the transmission of the energy carried by the first harmonic.

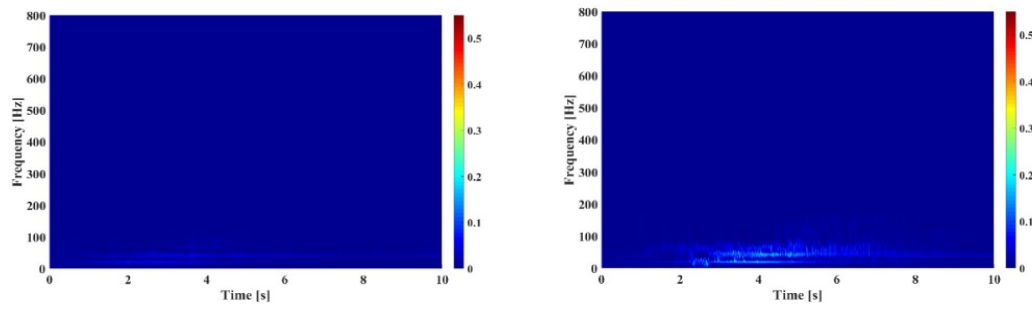


(a) Measuring Point 13

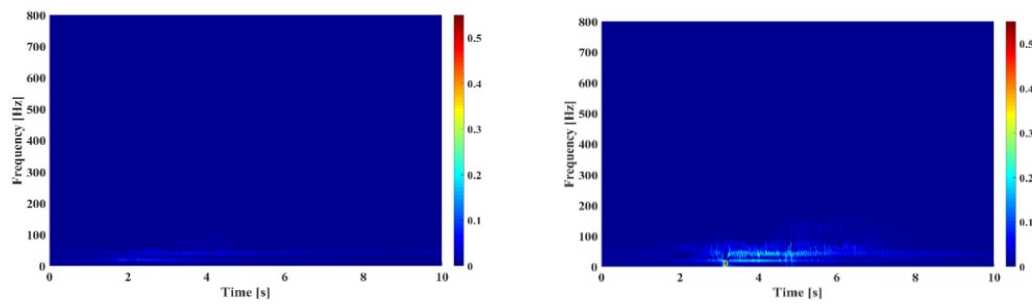
Figure 12. Cont.



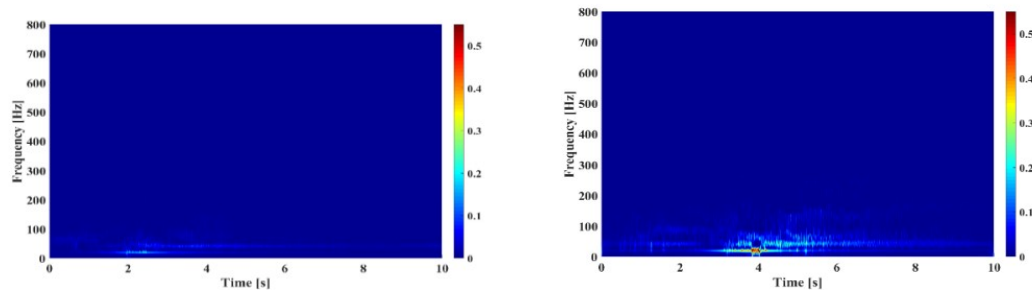
(b) Measuring Point 11



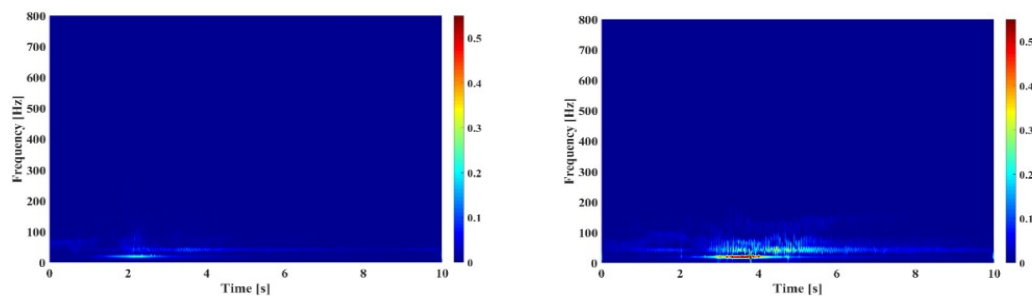
(c) Measuring Point 9



(d) Measuring Point 7



(e) Measuring Point 5



(f) Measuring Point 3

Figure 12. Cont.

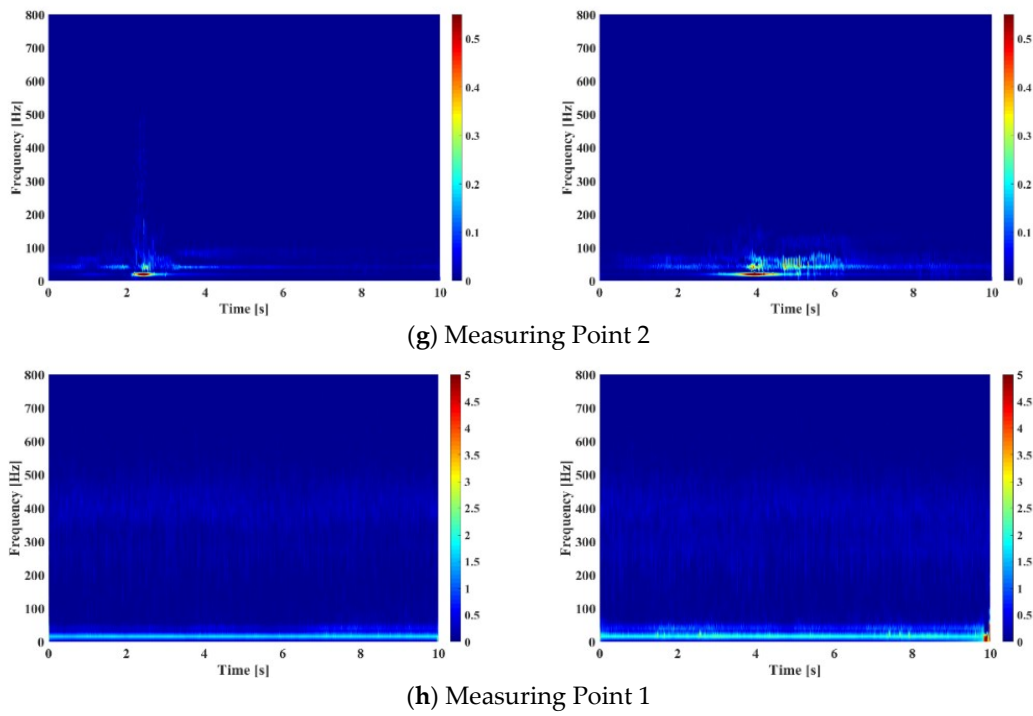


Figure 12. Hilbert energy spectrum of each measuring point in the first pass (left) and the eighth pass (right).

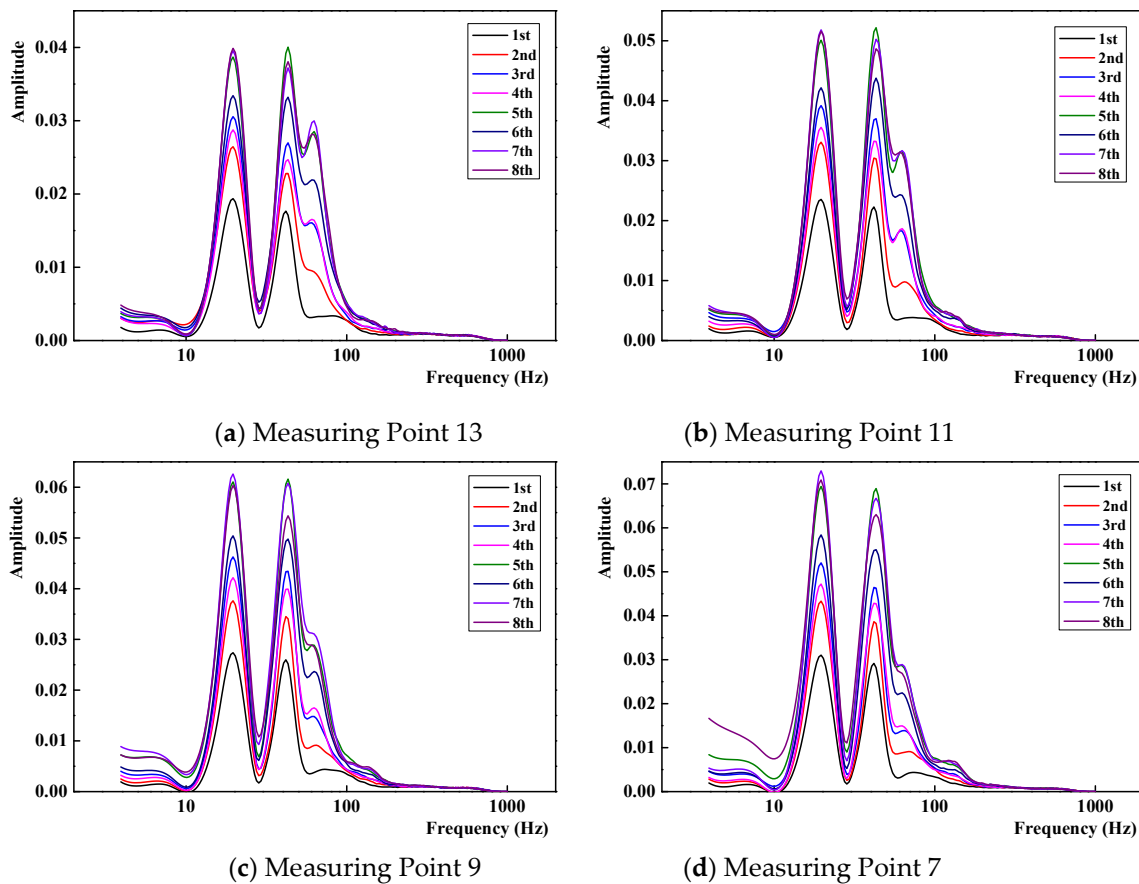


Figure 13. Cont.

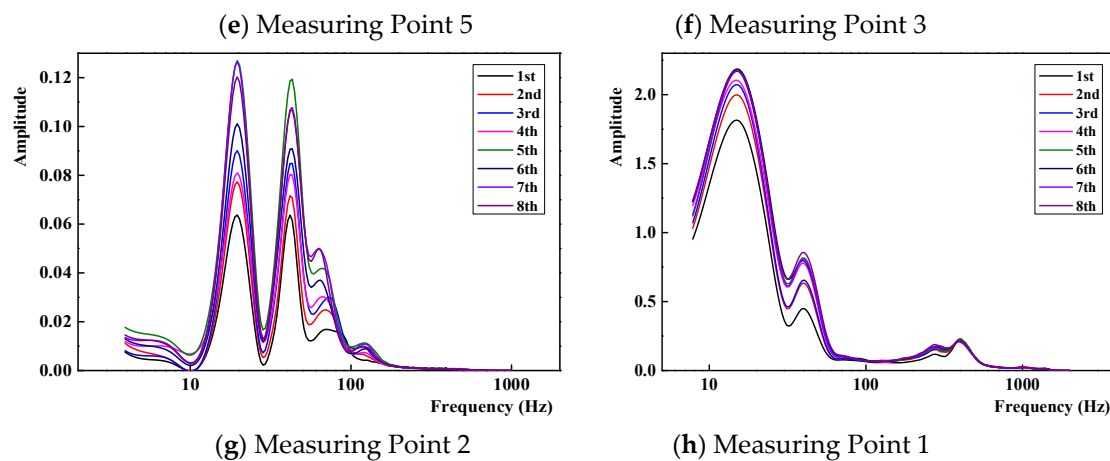


Figure 13. Hilbert marginal spectrum of each measuring point of wheel and filling materials.

4. Discussions

This paper selects one typical subgrade compaction project of Jingxiong Intercity Railway Gu'an Station to finish the research, some research results have been applied to the actual projects, such as the maximum rolling compaction times. However, the subgrade compaction is a very complicated, nonlinear dynamic progress, which involves the particle distributions and moisture content of filling materials, construction environment and so on. The results can provide some references for other similar engineering projects, but it needs to finish more research for its application.

5. Conclusions

Aiming at the shortages in exploring the transmission and evolution characteristics of the vibration signal, such as a few studies by using the jointed time–frequency domain and field prototypes tests, the typical subgrade compaction project of Jingxiong Intercity Railway Gu'an Station is selected to carry out the field prototypes tests, and the dynamic response from the vibratory roller to filling materials was monitored in the whole compaction process. Some efficient field tests data will be obtained. Based on this, the transmission and evolution characteristics of the vibration signal from the vibratory roller to filling materials in the compaction process are studied from time domain, frequency domain, jointed time–frequency domain and energy domain by using one new signal analysis technology, Hilbert–Huang Transform, which can relatively overall reveal the transmission and evolution mechanism of vibration wave. Some conclusions can be obtained as follows:

First, during the propagation of the vibration signal from wheel to filling materials, the vibration acceleration peak gradually decreases with the increase of buried depth, and when the buried depth reaches 1.8m, the vibration acceleration peak is closed to zero. At the same time, when the vibration wave propagates from wheel to the surface of the filling, the attenuation rate of acceleration gradually increases with the increase of rolling compaction times, while the attenuation rate of other layers in different buried depth gradually decreases.

Second, the vibration wave contains fundamental wave and multiple harmonics, and the dominant frequency of fundamental wave is nearly 21 Hz. With the increase of buried depth, the amplitude of fundamental, primary, secondary, until fifth harmonics decreases exponentially, and the concrete functional relationship among different amplitude of harmonics can be summarized as $y = Ae^{-BX}$. In the formula, A and B represent the coefficient, X represents the order of harmonic and Y represents the amplitude of harmonic when its order is X.

Third, the vibration energy focuses on the fundamental wave and primary wave, which can increase with the increase of rolling compaction times, and when the rolling compaction time reaches five, their energy reaches maximum. However, when the filling reaches a dense situation, the energy

of the primary wave gradually decreases. Therefore, the maximum rolling compaction time is five in the practical engineering applications.

Author Contributions: All authors contributed equally. C.Y. is the responsible person for field tests, proposed the research ideas. L.Z. is the site representative of field tests and help C.Y. to finish the modification in the revised manuscript. Y.H. finished the data process work and first version manuscript. D.C. provided the funding acquisition and help. S.W. helped Zhang Liang to finish the field tests. All authors have read and agreed to the published version of the manuscript.

Funding: This study is supported in part by National key research and development plan (No. 2018YFE0207100); Natural Science Foundation of China (Contract No. 41731288); Sichuan provincial science and technology support project (No. 18MZGC0186,18MZGC0247, 2018JY0549); China national railway group co. LTD Scientific Research Project (No. SY2016G003, N2019G002; P2019T001); CHINA ACADEMY OF RAILWAY SCIENCES CORPORATION LIMITED Research and development fund (No. 2019YJ026); 2017-2019 Young Elite Scientist Sponsorship Program by CAST. 2019 Young top talents Sponsorship Program of China Ten thousand people plan (No. 2019YJ300); 2018 Sichuan province Ten thousand people plan; Nanchang Railway Bureau Scientific Research Project (No. 20171106), and CHINA RAILWAY ERYUAN ENGINEERING GROUP CO.LTD Scientific Research Project (No. KYY2019145(19-20)).

Conflicts of Interest: The authors declare no conflicts of interest.

References

- Smith, R.A.; Zhou, J. Background of recent developments of passenger railways in China, the UK and other European countries. *J. Zhejiang Univ. Sci. A Appl. Phys. Eng.* **2014**, *15*, 925–935. [[CrossRef](#)]
- Zhang, J.L.; Xu, J.H.; Cai, Y. Research on quality inspection and control of continuous compacted subgrade. *Rock Soil Mech.* **2015**, *36*, 1141–1146.
- Liu, J.K.; Xiao, J.H. Experimental Study on the Stability of Railroad Silt Subgrade with Increasing Train Speed. *J. Geotech. Geoenviron. Eng.* **2010**, *136*, 833–841. [[CrossRef](#)]
- Cai, H.B.; Kuczek, T.; Dunston, P.S.; Li, S. Correlating Intelligent Compaction Data to In Situ Soil Compaction Quality Measurements. *J. Constr. Eng. Manag.* **2017**, *143*, 04017038. [[CrossRef](#)]
- Zhu, X.; Bai, S.; Xue, G.; Yang, J.; Cai, Y.S.; Hu, W.; Jia, X.Y.; Huang, B.S. Assessment of compaction quality of multi-layer pavement structure based on intelligent compaction technology. *Constr. Build. Mater.* **2018**, *161*, 316–329. [[CrossRef](#)]
- Hu, W.; Jia, X.Y.; Zhu, X.Y.; Gong, H.R.; Xue, G.P.; Huang, B.S. Investigating key factors of intelligent compaction for asphalt paving: A comparative case study. *Constr. Build. Mater.* **2019**, *229*, 116876. [[CrossRef](#)]
- Mooney, M.A. *Intelligent Soil Compaction Systems*; Transportation Research Board: Washington, DC, USA, 2010.
- Thurner, H.; Sandstr, M. Continuous compaction control. In Proceedings of the European Work Compaction of Soils and Granular Materials, Paris, France, 19 May 2000; pp. 237–246.
- White, D.; Thompson, M. Relationships between in situ and rollerintegrated compaction measurements for granular soils. *J. Geotech. Geoenviron. Eng.* **2008**, *134*, 1763–1770. [[CrossRef](#)]
- Nohse, Y.; Kitano, M. Development of a new type of single wheel vibratory roller. In Proceedings of the 14th International Conference of the International Society for Terrain-Vehicle Systems, Vicksburg, MS, USA, 20–24 October 2002; pp. 1–10.
- Mooney, M.A.; Rinehart, R.V. Instrumentation of a roller compactor to monitor vibration behavior during earthwork compaction. *J. Autom. Constr.* **2007**, *17*, 144–150.
- Thompson, M.; White, D. Field calibration and spatial analysis of compaction-monitoring technology measurements. *Transp. Res. Rec.* **2007**, *2004*, 69–79. [[CrossRef](#)]
- Liu, D.H.; Lin, M.; Li, S. Real-time quality monitoring and control of highway compaction. *Autom. Constr.* **2016**, *62*, 114–123. [[CrossRef](#)]
- Commuri, S.; Mai, A.T.; Zaman, M. Neural network-based intelligent compaction analyzer for estimating compaction quality of hot asphalt mixes. *J. Constr. Eng. Manag.* **2011**, *137*, 634–644. [[CrossRef](#)]
- Minchin, R.E., Jr.; Swanson, D.C.; Gruss, A.F.; Thomas, H.R. Computer applications in intelligent compaction. *J. Comput. Civ. Eng.* **2008**, *22*, 243–251. [[CrossRef](#)]
- Japan Society of Soil Engineering. *On-Site Compaction of Coarse Aggregates*; Guo, X.L., Wen, D., Eds.; Water&Power Press: Beijing, China, 1999.

17. Xu, G.H.; Gao, H.; Wang, W.Z. Continuous Dynamic Monitor Technology on Subgrade Compaction Quality. *China J. Highw. Transp.* **2007**, *20*, 17–22.
18. Hu, W.; Shu, X.; Jia, X.Y.; Huang, B.S. Geostatistical analysis of intelligent compaction measurements for asphalt pavement compaction. *Autom. Constr.* **2018**, *89*, 162–169. [[CrossRef](#)]
19. Imran, S.A. Monitoring of subgrade stiffness during compaction. *Transp. Res. Procedia* **2016**, 617–625. [[CrossRef](#)]
20. White, D.; Vennapusa, P.; Gieselmann, H. Field assessment and specification review for roller-integrated compaction monitoring technologies. *Adv. Civ. Eng.* **2011**, *2011*, 783836. [[CrossRef](#)]
21. Xu, Q.; Chang, G.K.; Gallivan, V.L. Development of a systematic method for intelligent compaction data analysis and management. *Constr. Build. Mater.* **2012**, *37*, 470–480. [[CrossRef](#)]
22. Adam, D. Roller-integrated Continuous Compaction Control (CCC) Technical Contractual Provisions & Recommendations. *Des. Constr. Pavements Rail Tracks* **2007**, *10*, 111–138.
23. Meehan, C.L.; Cacciola, D.V.; Tehrani, F.S.; Baker, W.J. Assessing soil compaction using continuous compaction control and location-specific in situ tests. *Autom. Constr.* **2017**, *73*, 31–44. [[CrossRef](#)]
24. KR Ber, W.; Floss, E.H.R.; Wallrath, W. Dynamic soil stiffness as quality criterion for soil compaction. In *Geotechnics for Roads, Rail Tracks, and Earth Structure*; Balkema: Rotterdam, The Netherlands, 2001; pp. 189–199.
25. Kumar, S.A.; Aldouri, R.; Nazarian, S.; Si, J. Accelerated assessment of quality of compacted geomaterials with intelligent compaction technology. *Constr. Build. Mater.* **2016**, *113*, 824–834. [[CrossRef](#)]
26. Suits, L.D.; Sheahan, T.C.; Facas, N.W. Development and Evaluation of Relative Compaction Specifications Using Roller-Based Measurements. *Geotech. Test. J.* **2011**, *34*, 102915. [[CrossRef](#)]
27. He, M.; Li, L.; Nie, Z. Experimental research of dynamic continuous compaction control of subgrade compaction. *J. Beijing Jiaotong Univ.* **2010**, *6*, 7.
28. Jiao, T.; Wang, X.; Huang, Y.B. Stability Control of Continuous Compaction Measurement in High-Speed Railway Subgrade. *Appl. Mech. Mater.* **2013**, *438–439*, 1104–1107. [[CrossRef](#)]
29. Pistor, J.; Villwock, S.; Völkel, W.; Kopf, F.; Adam, D. Continuous Compaction Control (CCC) with Oscillating Rollers. *Procedia Eng.* **2016**, *143*, 514–521. [[CrossRef](#)]
30. Brandl, H.; Adam, D. Sophisticated continuous compaction control of soils and granular materials. In *Proceedings of the 14th International Conference on Soil Mechanics and Foundation Engineering*, Balkema, Rotterdam, The Netherlands, 6 September 1997; pp. 1–6.
31. Barman, M.; Nazari, M.; Imran, S.A.; Commuri, S.; Zaman, M.; Beainy, F.; Singh, D. Quality control of subgrade soil using intelligent compaction. *Innov. Infrastruct. Solut.* **2016**, *1*, 23. [[CrossRef](#)]
32. Rinehart, R.V.; Mooney, M.A.; Facas, N.F.; Musimbi, O.M. Examination of Roller-Integrated Continuous Compaction Control on Colorado Test Site. *Transp. Res. Rec.* **2012**, *2310*, 3–9. [[CrossRef](#)]
33. Mooney, M.A.; Rinehart, R.V. Field Monitoring of Roller Vibration during Compaction of Subgrade Soil. *J. Geotech. Geoenviron. Eng.* **2007**, *133*, 257–265. [[CrossRef](#)]
34. Mooney, M.A.; Gorman, P.B.; Gonzalez, J.N. Vibration based health monitoring of earth structures. *Struct. Health Monit.* **2005**, *4*, 137–152. [[CrossRef](#)]
35. Herrera, C.; Alves Costa, P.; Caicedo, B. Numerical modelling and inverse analysis of continuous compaction control. *Transp. Geotech.* **2018**, *17*, 165–177. [[CrossRef](#)]
36. Pietzsch, D.; Poppy, W. Simulation of soil compaction with vibratory rollers. *J. Terramech.* **1992**, *29*, 585–597. [[CrossRef](#)]
37. Lee, J.N.; Tsai, Y.C.; Chen, H.S.; Kung, H.K. An Integrated Approach of CAD/CAM for Spatial Cam with Oscillating Cylindrical Rollers. *Adv. Mater. Res.* **2011**, *201–203*, 318–325. [[CrossRef](#)]
38. Heersink, D.K.; Furrer, R. Sequential spatial analysis of large datasets with applications to modern earthwork compaction roller measurement values. *Spat. Stat.* **2013**, *6*, 41–56. [[CrossRef](#)]
39. Yu, Q.M.; Liu, J.K.; Tian, Y.H. Analysis of Application Situation of Continuous Compaction Control (CCC). *Appl. Mech. Mater.* **2014**, *501–504*, 983–992. [[CrossRef](#)]
40. Nie, Z.H.; Wang, X.; Jiao, T. Anomalous Data Detection for Roller-Integrated Compaction Measurement. *Int. J. Geomech.* **2016**, *16*, B4015004. [[CrossRef](#)]
41. Ning, J.L.; Cao, Y.W. A new method for continuous detection of compaction. *J. Chongqing Jiaotong Univ. Nat. Sci.* **2007**, *26*, 74–77.

42. Gao, F.Y.; Ji, C.; Long, Y.; Song, K.J. Dynamic responses and damages of water-filled cylindrical shell subjected to explosion impact laterally. *J. Lat. Am. J. Solids Struct.* **2014**, *11*, 1924–1940. [[CrossRef](#)]
43. Huang, N.E. Introduction to the Hilbert-Huang transform and its related mathematical problems. *Interdiscip. Math.* **2005**. [[CrossRef](#)]
44. Huang, N.E.; Shen, Z.; Long, S.R.; Wu, M.C.; Shih, H.H.; Zheng, Q.; Yen, N.-C.; Tungand, C.C.; Liu, H.H. The empirical mode decomposition and the Hilbert spectrum for nonlinear and non-stationary time series analysis. *Proc. A* **1998**, *454*, 903–995. [[CrossRef](#)]
45. Huang, N.E.; Wu, Z. A review on Hilbert-Huang transform: Method and its applications to geophysical studies. *Rev. Geophys.* **2008**, *46*. [[CrossRef](#)]



© 2020 by the authors. Licensee MDPI, Basel, Switzerland. This article is an open access article distributed under the terms and conditions of the Creative Commons Attribution (CC BY) license (<http://creativecommons.org/licenses/by/4.0/>).